Top Yukawa coupling measurement with indefinite *CP* Higgs in $e^+e^- \to t\bar{t}\Phi$

B. Ananthanarayan,[1,*] Sumit K. Garg,[2,†] C. S. Kim,[2,‡] Jayita Lahiri,[1,§] and P. Poulose[3,‖]

[1]*Centre for High Energy Physics, Indian Institute of Science, Bangalore 560 012, India*
[2]*Department of Physics and IPAP, Yonsei University, Seoul 120-749, Korea*
[3]*Department of Physics, Indian Institute of Technology Guwahati, Guwahati 781 039, India*

(Received 27 May 2014; published 10 July 2014)

We consider the issue of the top quark Yukawa coupling measurement in a model-independent and general case with the inclusion of *CP* violation in the coupling. Arguably the best process to study this coupling is the associated production of the Higgs boson along with a $t\bar{t}$ pair in a machine like the International Linear Collider (ILC). While detailed analyses of the sensitivity of the measurement—assuming a Standard Model (SM)-like coupling is available in the context of the ILC—conclude that the coupling could be pinned down to about a 10% level with modest luminosity, our investigations show that the scenario could be different in the case of a more general coupling. The modified Lorentz structure resulting in a changed functional dependence of the cross section on the coupling, along with the difference in the cross section itself leads to considerable deviation in the sensitivity. Our studies of the ILC with center-of-mass energies of 500 GeV, 800 GeV, and 1000 GeV show that moderate *CP* mixing in the Higgs sector could change the sensitivity to about 20%, while it could be worsened to 75% in cases which could accommodate more dramatic changes in the coupling. Detailed considerations of the decay distributions point to a need for a relook at the analysis strategy followed for the case of the SM, such as for a model-independent analysis of the top quark Yukawa coupling measurement. This study strongly suggests that a joint analysis of the *CP* properties and the Yukawa coupling measurement would be the way forward at the ILC and that caution must be exercised in the measurement of the Yukawa couplings and the conclusions drawn from it.

DOI: 10.1103/PhysRevD.90.014016 PACS numbers: 13.66.-a, 12.60.-i, 13.88.+e, 12.60.Fr

I. INTRODUCTION

The recent discovery of a Higgs-like particle by the Large Hadron Collider (LHC), weighing about 125 GeV/c^2 [1–7], quite positively indicates that the Higgs mechanism is at work to bring in electroweak symmetry breaking, thus providing mass to the elementary particles. While one of the parameters, namely the mass of the new particle, is somewhat precisely determined in different detection channels and by two independent experiments, one needs to go a long way before establishing the full identity of this particle, in terms of its couplings to other particles, as well as in terms of its constitution. At the same time, the reasons to look beyond the SM will not be diminished, even if the new resonance has all the properties as expected within the SM. For example, concerning the Higgs sector, one will still need to cure the quadratically divergent quantum corrections to the mass of the standard Higgs boson. The other reasons include the existence of dark matter, the existence of neutrino masses, baryon asymmetry, etc., which clearly indicate the need to look beyond the SM. Indeed, the newly discovered particle, with the understanding of its properties, will provide the much needed handle in the search beyond the SM. With the limitations of a hadronic machine, the LHC may not be able to exhaustively study the properties of the new resonance.[1] On the other hand, the clean environment of the proposed International Linear Collider (ILC) [12,13], which is an e^+e^- collider, will help us to carry out precision experiments on elementary particles and establish their properties, including that of the purported Higgs boson, which here we shall denote by Φ. The possibility of beam polarization could significantly enhance the sensitivity of the ILC in general, and also allow us to probe beyond the SM signals [14].

The process that is of interest to us in this work is

$$e^+e^- \to t\bar{t}\Phi. \tag{1}$$

This process is, by definition, key to the measurement of the top quark Yukawa coupling to the Higgs. The Feynman diagrams, at tree level, corresponding to this process are given in Fig. 1. This includes the Higgs-strahlung process (with $ZZ\Phi$ coupling), the contribution of which to the total cross section is about 5%. We invite the attention of the reader to Refs. [15–17] and references therein for some

*anant@cts.iisc.ernet.in
†aslv15@gmail.com
‡cskim@yonsei.ac.kr
§jayita@cts.iisc.ernet.in
‖poulose@iitg.ernet.in

[1]Refer to Refs. [8–11] for some of the studies of top Higgs Yukawa couplings in the context of the LHC.

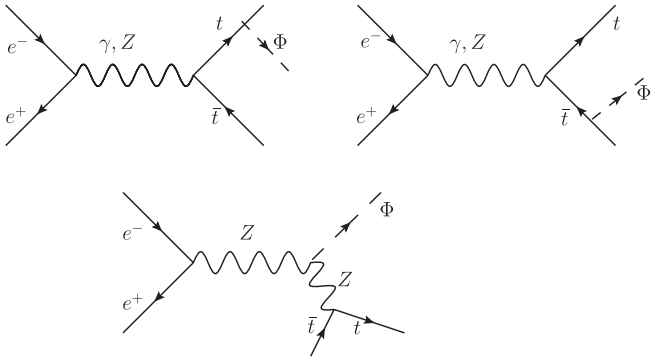

FIG. 1. Feynman diagrams contributing to the process $e^-e^+ \to t\bar{t}\Phi$ in the Standard Model.

early work on this topic. More recently, the process has attracted renewed attention in Refs. [18,19], which present a detailed analysis of the background involved and the feasibility of the ILC to measure the top Yukawa coupling, concluding that the ILC at an 800 GeV center-of-mass energy is best suited for such measurement. The issue of threshold corrections due to $t\bar{t}$ bound-state effects, more relevant at a center-of-mass energy close to 500 GeV, are considered in some detail in Refs. [20,21], which also carry out detailed and sophisticated analysis, including considerations of the signal and backgrounds in various channels, with the help of prototype ILC event generators, and making use of the beam polarization. Restricted within the SM, these studies have established that the top quark Yukawa coupling could be measured with an accuracy of about 10%. The direct measurement of the coupling, using the semileptonic decays of the W's coming from the top quarks, is considered in Ref. [22], which concludes that the accuracy of the determination of the coupling is about 30%. The guiding relation between the limit with which the Yukawa coupling (g_t^M) can be measured and that of the cross section (σ) is [23]

$$\frac{\Delta g_t^M}{g_t^M} = \left(\frac{\sigma/g_t}{|d\sigma/dg_t|}\right)_{g_t=g_t^M} \frac{\Delta\sigma}{\sigma}, \tag{2}$$

where g_t is considered as a variable, and g_t^{M} is the top Yukawa coupling for the model under consideration, which is to be evaluated at the top mass, $m_t = 173.5$ GeV. It may be noted that, while $\Delta\sigma$ depends on the details of the experimental efficiency of isolating the signal over the background, apart from detection efficiencies relevant to the final states involved, the prefactor $\left(\frac{\sigma/g_t}{|d\sigma/dg_t|}\right)_{g_t=g_t^M}$ depends crucially on how the cross section depends on g_t. It is easily imagined in a beyond-the-SM (BSM) scenario with multiple Higgs fields participating in electroweak symmetry breaking (EWSB), to have the functional dependence of the cross section on the Yukawa coupling different from that in the SM [24]. For example, cases with CP-mixed Higgs bosons will have a $t\bar{t}\Phi$ coupling with a different Lorentz structure than that of the SM, which can complicate the dependence.[2] *A priori*, it is not clear what kind of differences are expected in the prefactor in the presence of anomalous couplings, compared to the SM case. Neither is it clear if the signal significance remains the same in both cases. It is the purpose of this work to attempt to answer this question, without getting into the detailed analysis.

While it has been reported by the LHC collaborations that the new resonance is very likely a scalar, the spin and parity studies so far are very limited. Investigating the case of a scalar-pseudoscalar admixture should involve a different strategy than what has been adopted so far. Most of the multi-Higgs models, including the two-Higgs-doublet model (2HDM), and the minimal and next-to-minimal superpsymmetric Standard Models (MSSM and NMSSM), are some of the popular extensions of the SM with CP-odd as well as CP-even scalar particles in their CP-conserving versions. Inclusion of CP violation in the Higgs sector of such models allows CP-mixed physical scalars. The phenomenology of such a possibility has been considered in the literature [26–30]. In a recent study [31], it has been pointed out that the ILC is an ideal setting to probe the CP nature of the Higgs boson in the process considered here. It is clear that the scalar and pseudoscalar parts of a CP-mixed Higgs boson will couple differently to different polarization combinations of the top quark and top antiquark. Suitable observables involving top quark polarization, such as polarization asymmetry, could therefore probe the CP nature of the Higgs boson through this process. With the combined use of the total cross section, its energy dependence, the polarization asymmetry of the top quark, and the up-down asymmetry of the antitop with respect to the top quark–electron plane, Ref. [32] has shown that the CP properties can be efficiently probed through the same process of $t\bar{t}\Phi$ production at the ILC. An early approach complementary to these works is Ref. [33]. The other process being scrutinized to investigate the CP nature of the Higgs is $e^+e^- \to Z\Phi$, with the Higgs boson decaying to τ-lepton pairs [34–36]. A general case of model-independent effective anomalous couplings is studied by Ref. [37].

In our recent work [38], we have studied the possibility of fingerprinting the departure from the CP-even case in decay distributions of the process in Eq. (1). In this study, two definite scenarios, which we denote as model I and model II, have been considered. Model I corresponds to the minimal extension of the SM with one additional pseudoscalar degree of freedom, which mixes with the SM scalar to form the physical Higgs boson [31]. This model is characterized by one free parameter, and the $t\bar{t}$ couplings to scalar and pseudoscalar are related by a sum rule that the sum of the squares of the couplings is the same as that of the square of the SM coupling. Similarly, the $ZZ\Phi$ coupling

[2]For an early review, please see Ref. [25].

is scaled by the same parameter that scales the scalar coupling to $t\bar{t}$, as the gauge bosons do not couple to pseudoscalars at tree level. Model II is a more realistic case, similar to the CP-violating 2HDM model, which has some essential features that make it quite different from model I. In particular, there is no theoretical constraint (sum rule) on the parameters, and the scaling of the $ZZ\Phi$ coupling is not necessarily scaled by the same parameter that scales the scalar coupling to $t\bar{t}$, which is true in general in multi-Higgs models with more than one Higgs field transforming nontrivially under $SU(2)_L$. Confining ourselves to some reasonable ranges of these parameters guided by the experimental indications that the new resonance is close to a CP-even case, we consider the effect of a CP-violating Higgs boson in the decay spectrum of both the top quark and the Higgs boson itself, noting that the decay distributions are the spin analyzers of the parent particle. In view of the remarks above, it is a natural extension of this work to understand the impact of such a CP-indefinite Higgs boson on the top quark Yukawa coupling measurement. In the present work we address this issue. In order to perform numerical analysis, we have used the integrated Monte Carlo and event generation package WHIZARD [39], which incorporates the SM, as well as some of its popular extensions. Further, WHIZARD also allows us to incorporate any new model described by a Lagrangian, through an interface [40] generated using FEYNRULES [41]. In particular, for our analysis, we have considered a suitably modified version of the model including the anomalous $tt\Phi$ coupling, as prescribed by models I and II mentioned above.

The scheme of this paper is as follows: In Sec. II, we introduce and describe the basic structure of an indefinite CP Higgs sector in the two scenarios mentioned above. In Sec. III, we describe the processes we consider. In Sec. IV, we present the results of our analysis. In Sec. V, we present a discussion and our conclusions.

II. TOP YUKAWA COUPLING

Since the discovery of the Higgs boson, studying its properties in much detail is the foremost task, which will further establish the Higgs symmetry-breaking mechanism. The Standard Model contains one Higgs doublet, which by acquiring its vacuum expectation value (VEV), results in a CP-even physical scalar field. The heaviness of the top quark makes it possible to study the fermion-Higgs interactions at the production level, augmenting to the possibilities through the fermionic decay channels. In the SM, the strength of Yukawa couplings to fermions at tree level is given by

$$g_{f\bar{f}\Phi} = M_f/v, \tag{3}$$

where $v = 246$ GeV is the vacuum expectation value and M_f is the mass of the fermion. For a top quark of mass $M_t = 174$ GeV, the Yukawa coupling is given by $y_{t\bar{t}\Phi} = 0.71$. QCD and weak corrections to this coupling are estimated to be about 10%. While this is so, there are compelling reasons to look beyond the SM, as indicated in the Introduction. Many of the scenarios proposed to go beyond the SM have a more complex Higgs sector, offering possibilities of more than one physical Higgs boson. In the CP-conserving scenarios, some of these are scalar particles and some are pseudoscalar particles, while in the CP-violating cases, the scalar-pseudoscalar mixing could result in CP-indefinite Higgs bosons. For example, in one of the minimal extensions of the Higgs sector beyond the SM, an additional $SU(2)_L$ doublet field is introduced in the two-Higgs-doublet model (2HDM), resulting in five physical Higgs bosons, one of which is a CP-odd neutral particle. In such multi-Higgs scenarios, the Yukawa coupling is in general expected to be different from that of the SM case. While in the CP-conserving cases, there could maximally be a scaling of the Yukawa coupling compared to its SM value, in the CP-violating cases, there is a different Lorentz structure involved in the coupling. Such a CP-indefinite state will also couple differently to the gauge bosons. Concerning the present study, we shall focus on the $t\bar{t}\Phi$ production at the ILC, relevant to which both the $t\bar{t}\Phi$ and the $ZZ\Phi$ couplings take a form which may be parametrized as follows [31,37]:

$$g_{t\bar{t}\Phi} = -i\frac{e}{s_W}\frac{m_t}{2M_W}(a + ib\gamma_5),$$
$$g^{\mu\nu}_{ZZ\Phi} = -ic\frac{eM_Z}{s_W c_W}g^{\mu\nu}. \tag{4}$$

Here, $s_W \equiv \sin\theta_W (= \sqrt{1 - c_W^2})$, where θ_W is the Weinberg angle. In the SM with only one scalar Higgs Boson (h), the parameters take the values $a = 1$, $b = 0$, and $c = 1$. In specific models, all these parameters may not be independent. In the following, we will describe two simple scenarios that are phenomenologically viable and can be linked to some of the popular extensions of the SM.

A. Model I

One of the most simple and straightforward extensions of the Higgs sector of the SM to incorporate CP violation is to imagine the presence of an additional pseudoscalar degree of freedom (A), which mixes with the scalar degree of freedom to produce a physical state:

$$\begin{pmatrix}\Phi\\ \chi\end{pmatrix} = \begin{pmatrix}\cos\theta & \sin\theta\\ \sin\theta & \cos\theta\end{pmatrix}\begin{pmatrix}h\\ A\end{pmatrix}. \tag{5}$$

Considering Φ as the 125 GeV resonance[3] being under investigation here, the parameters a and b above are identified as $a = \cos\theta$ and $b = \sin\theta$, which are now constrained by

[3]The orthogonal combination, χ, could be imagined to be heavy, and therefore does not interfere with the phenomenology at the energy scales we consider.

$$a^2 + b^2 = 1. \tag{6}$$

Since the SM gauge boson Z does not couple to the pseudoscalar degree of freedom, we have $c = a$ in this scenario. The down-type quarks as well as the charged leptons will also have the same coupling structure as the up-type quarks, so that, for example, the b-quark coupling becomes

$$g_{\Phi bb} = -i\frac{e}{s_W}\frac{m_b}{2M_W}(a + ib\gamma_5). \tag{7}$$

In the following, we call this scenario "model I." The advantage here is that there is only one additional parameter to deal with, making it very friendly to perform phenomenological investigations. The disadvantage is that most of the realistic extensions of the SM with multi-Higgs scenarios have more complex Higgs sectors, which do not support the above constraint.

B. Model II

In more realistic extentions of the SM, the Higgs sector allows a more relaxed assignment of the parameter values compared to the scenario in model I above.

In a completely model-independent approach, we can treat the parameters a, b to be independent of each other. Some specific cases of this scenario are the 2HDM and MSSM with CP violation where there are two Higgs doublet fields, leading to two neutral scalar bosons and one neutral pseudoscalar boson which could mix with each other. Thus, the physical mass eigenstates are given as

$$\begin{pmatrix}\phi_1\\ \phi_2\\ A\end{pmatrix} = \mathcal{O}_{3\times 3}\begin{pmatrix}H_1\\ H_2\\ H_3\end{pmatrix}, \tag{8}$$

where ϕ_1 and ϕ_2 are the scalar gauge eigenstates, and A is the pseudoscalar gauge eigenstate [42]. This, in effect, removes the restricting relations between the parameters a, b, and c. For ready reference, we take the example of the MSSM case (or 2HDM) with CP violation in the Higgs sector. The couplings of the Higgs boson with the fermions and the gauge bosons, where $\tan\beta$ is the ratio of the VEVs of the two Higgs fields, are given by

$$\begin{aligned}\text{top quark}:\ & a_u = \mathcal{O}_{2i}/\sin\beta, \qquad b_u = -\mathcal{O}_{3i}\cot\beta;\\ \text{bottom quark}/\tau\text{-lepton}:\ & a_d = \mathcal{O}_{1i}/\cos\beta, \qquad b_d = -\mathcal{O}_{3i}\tan\beta;\\ \text{gauge bosons}:\ & c = \mathcal{O}_{1i}\cos\beta + \mathcal{O}_{2i}\sin\beta;\end{aligned} \tag{9}$$

where we have introduced the subscripts u and d on the parameters a and b to denote the up-type and down-type quarks, respectively. The mixing matrix elements satisfy the normalization conditions:

$$\mathcal{O}_{1i}^2 + \mathcal{O}_{2i}^2 + \mathcal{O}_{3i}^2 = 1. \tag{10}$$

We call this scenario "model II" in the rest of this article.

The lightest of the Higgs bosons, H_1, could be assumed to be the discovered 125 GeV resonance (denoted by Φ), while H_2 and H_3 are considered to be heavy enough to be out of the LHC's range investigated so far.

As mentioned in the Introduction, it will be a little premature to make conclusions regarding the CP properties of the new resonance from the LHC results so far. It can accommodate some amount of scalar-pseudoscalar mixing within specific models like the 2HDM, MSSM, and NMSSM with a CP-violating Higgs sector. However, the amount of mixing in these models is highly constrained mainly by the results from the flavor sector, as well as the atomic electric dipole moments measurements [43,44]. At the same time, it is possible to have large values for the parameters a and b even when the CP-odd component of the physical Higgs boson is small [38]. In the present work, we do not intend to consider any specific model, as the viability of such models and the restrictions on their parameters depend on many constraints outside the considerations of the Higgs sector itself. Instead, we will take a model-independent approach, letting the relevant parameters (a, b, and c) be rather free, but at the same time keeping them within a small range, without any further justification.

In the following sections, we will analyze the effect of the anomalous couplings, employed through the scenarios presented above, in the top quark Yukawa coupling measurements.

III. ANALYSIS METHODOLOGY

The process under scrutiny is the associated production of the Higgs boson with a $t\bar{t}$ pair in e^+e^- collision. As explicitly shown in the Feynman diagrams in Fig. 1, this process proceeds through Higgs radiation off the top quarks, or through the Higgs-strahlung off the Z boson. Assuming the eeZ/γ couplings to be standard, the process receives contributions from new physics through the anomalous couplings $tt\Phi$ and $ZZ\Phi$. Keeping in focus the main goal of this study—namely, understanding the role of anomalous $tt\Phi$ and $ZZ\Phi$ couplings in the determination of top quark Yukawa couplings—we will follow the analysis strategy adopted in the proposed top quark Yukawa measurements, as in Refs. [20,21]. The strategy

there was to use Eq. (2) to determine the sensitivity of the coupling. It involves the determination of two quantities:

(i) The prefactor, $(\frac{\sigma/g_t}{|d\sigma/dg_t|})g_t = g_t^M$, is determined from the slope of the σ vs g_t curve. The cross section $\sigma_{t\bar{t}\Phi} \propto g_t^2$ when the contribution of Higgs-strahlung off the Z boson is neglected, leading to a prefactor value of $1/2$. The inclusion of the Higgs-strahlung modifies this by about 4% to 0.52 [20,21]. In general, the prefactor is determined by the functional dependence of the cross section on the Yukawa coupling.

(ii) The other factor in Eq. (2) is $\Delta\sigma/\sigma = \sqrt{S+B}/S$, where S is the number of signal events, and B is the number of background events. Getting the best (smallest) value for $\frac{\Delta\sigma}{\sigma}$ is a matter of experimental efficiency and a suitable choice of the observables at hand to reduce the background over the signal.

We will first assume that the strategy adopted by Refs. [20,21] to reduce the background and enhance the signal significance through the kinematic cuts on suitable variables considered therein is acceptable as it is, even in the presence of anomalous couplings. Further, we will consider various kinematic distributions comparing the case of SM and the case of anomalous couplings with the parameters assuming different values. Such a comparison is expected to indicate if the above assumptions regarding signal significance are realistic or not. This is important, as a detailed study of the signal and background, event reconstruction, and machine and detector efficiency specific to ILC, etc., is beyond the scope of this study, and therefore not attempted. Rather, we will be satisfied with a qualitative analysis of the various distributions of the signal with anomalous couplings.

Considering the signal process, we first discuss the different final states possible through different decay channels of $tt\Phi$. We note that, while the top quak decays almost 100% into Wb, the Higgs boson of mass 125 GeV could go through $b\bar{b}$, WW^*, and $\tau^+\tau^-$ with branching fractions (BR) of 57.7%, 21.5%, and 6.32%, respectively, in the SM. In our analysis, we consider the $b\bar{b}$ channel alone. This leaves the following distinct final states, depending on the decay channel of W:

(i) *Pure hadronic mode.*—In this mode, both the W's decay hadronically (BR = 45.6%), resulting in 4 jets + 4 b's in the final state:

$$e^-e^+ \to t\bar{t}\Phi \to W^+W^-b\bar{b}\Phi \to q_1\bar{q}_1'q_2\bar{q}_2'bb\bar{b}\,\bar{b}\,.$$

(ii) *Semileptonic mode.*—In this mode, one of the W's decays hadronically, while the other decays leptonically (BR = 43.9%), resulting in 2 jets + 4 b's + 1 lepton + E_{missing} in the final state:

$$e^-e^+ \to t\bar{t}\Phi \to W^+W^-b\bar{b}\Phi \to q_1\bar{q}_1'l\nu bb\bar{b}\,\bar{b}\,.$$

(iii) *Leptonic mode.*—In this mode, both the W's decay leptonically (BR = 10.5%), resulting in 4 b's + 2 leptons + E_{missing} in the final state:

$$e^-e^+ \to t\bar{t}\Phi \to W^+W^-b\bar{b}\Phi \to l\bar{l}\nu\bar{\nu}bb\bar{b}\,\bar{b}\,.$$

In the leptonic decays of the W, we have included only the channels with electrons and muons, keeping aside the tau decay channel. We have also assumed that b tagging can be performed with high efficiency, and thus b jets are distinguished from the lighter quark jets. In our further discussion, we include the hadronic and semileptonic modes, leaving out the purely leptonic channel, owing to its very small BR, and two missing particles in the final state. This is the strategy followed in other studies of top quark Yukawa coupling measurement through the same process.

Coming to the background, $t\bar{t}Z$ and $t\bar{t}g^*$, with a pair of b jets coming from Z and g^*, contribute to the irreducible backgrounds in the corresponding cases. Owing to the large cross section, the $t\bar{t}$ pair production could also give rise to the background, through event misconstruction.

We will now turn to our numerical studies in the next section.

IV. NUMERICAL RESULTS

For our numerical study, we considered the event generator, WHIZARD [39], with the model files suitably modified[4] to accommodate the anomalous couplings being studied, viz. $f\bar{f}\Phi$ and $VV\Phi$ couplings, where $f = t, b, \tau$ and $V = Z, W$, parametrized through Eqs. (4) and (7). We have cross-checked the correctness of our implementation by verifying the results of Ref. [31] for the process being scrutinized.

To examine the effect of anomalous couplings on the process, and thus in deriving the Yukawa couplings, we consider the following values of the parameters in the two scenarios presented in the previous section.

(i) *Model I.*—The only parameter in this scenario is denoted by b, which can assume any value in the range $0-1$. Specifically, we have considered $b = 0, 0.1, 0.3, 0.5$, and 0.7 for illustration, where $b = 0$ corresponds to the SM.

(ii) *Model II.*—As mentioned earlier, we consider a model-independent approach in this scenario, with the parameters allowed to vary independently of each other. While this is so, we have kept in mind the most likely possibility with the physical Higgs particle being mostly CP even, and therefore, c is close to unity. At the same time, a and b can be quite

[4]We refer to http://feynrules.irmp.ucl.ac.be/wiki/StandardModel in this regard.

TABLE I. Benchmark points in the case of model II.

	Z, W	Top		b/τ	
Point	c	a_u	b_u	a_d	b_d
P1	0.97	1.08	−0.05	0.5	−0.20
P2	0.93	0.82	−0.45	1.0	−0.29
P3	0.93	0.5	−1.0	0.5	−1.0
P4	0.93	−1.0	1.0	−1.0	1.0
P5	0.93	−1.0	−1.0	−1.0	−1.0
P6	0.93	1.0	1.0	1.0	1.0
P7	−0.93	1.0	1.0	1.0	1.0

different, and can be larger than 1. Although we do not follow any particular model, in order to be close to realistic cases, we have chosen the first benchmark point from *CP*-violating MSSM [38] and the second one from *CP*-violating 2HDM (type II, without SUSY) [45]. Both P1 and P2 have the parameters a and c positive, while b is negative. This seems to be the preferred direction in the case of the specific models considered. It is quite natural to ask what is the effect of the signs on these parameters on the cross section and other observables, and the conclusions drawn from those. To this effect, we consider a few other benchmark points (BP), somewhat arbitrarily, with different sign combinations. In Table I, we present the values of the parameters corresponding to these BPs.

Considering the effect of the anomalous couplings in the total cross section, in Fig. 2 we present the cross section against the center-of-mass energy for different values of b in the case of model I, and for the BPs considered, in the case of model II. In the case of model I, with a 30% pseudoscalar component ($b = 0.3$), there is about a 10% decrease in the cross section at the peak value, corresponding to a center-of-mass energy of 800 GeV. This is increased to about 40% with a 70% pseudoscalar component. Coming to model II, a_d and b_d do not affect the production process. They only leave their signature in the decay of the Higgs boson. With P1 and P2, there is a substantial difference in the cross section compared to the SM value, with the former having an enhanced effect, while the latter has a diminishing effect. This shows that the effect of the parameter a is somewhat dominating compared to that of the b parameter. The behavior of the cases of P4 and P5 clearly indicates that the sign of b has no perceivable effect in the total cross section. At the same time, a distinguishable effect of the sign of a is visible when comparing the points P4 and P6. Indeed, this is expected to be due to the interference between the diagram involving the $ZZ\Phi$ coupling and the others. In order to ascertain this, the signs of a and c are switched between P4 and P7, still keeping a relative negative sign. A comparison of P1 and P3 also brings out the different $\sqrt{s}$ behavior of the dependence of a and b. While the effect of a does not indicate any considerable change as the $\sqrt{s}$ is changed, in the case of b, the effects are substantially larger at larger $\sqrt{s}$. This advocates that an investigation of the process at a few chosen center-of-mass energy values will be more enlightening compared to an analysis sitting at only one center of mass-energy. Between P4 and P7, the signs of a and c are switched, so as to keep a relative negative sign.

In order to understand how the above mentioned differences affect the Yukawa coupling measurement, we first focus on the case of the ILC running at a center-of-mass energy of 800 GeV, as the cross section peaks around this value. The cases of 500 GeV and 1000 GeV are also included so as to see the effect of the $\sqrt{s}$ dependence. In the rest of this section, we shall consider each of these cases separately and discuss the effect of the anomalous

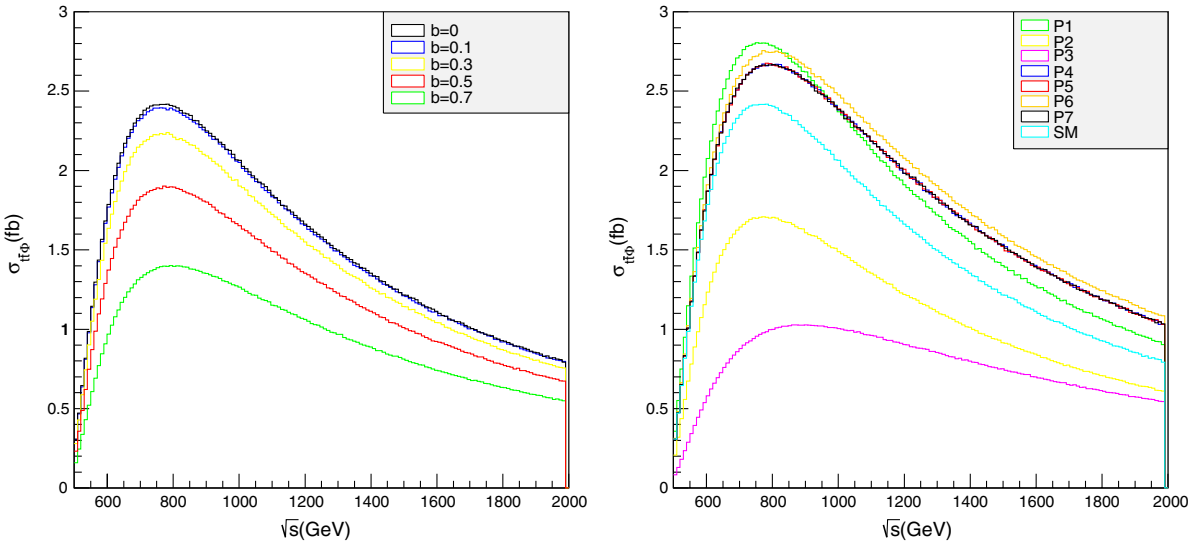

FIG. 2 (color online). $\sigma_{t\bar{t}\Phi}$ vs $\sqrt{s}$ for different parameter values in model I (left panel) and model II (right panel).

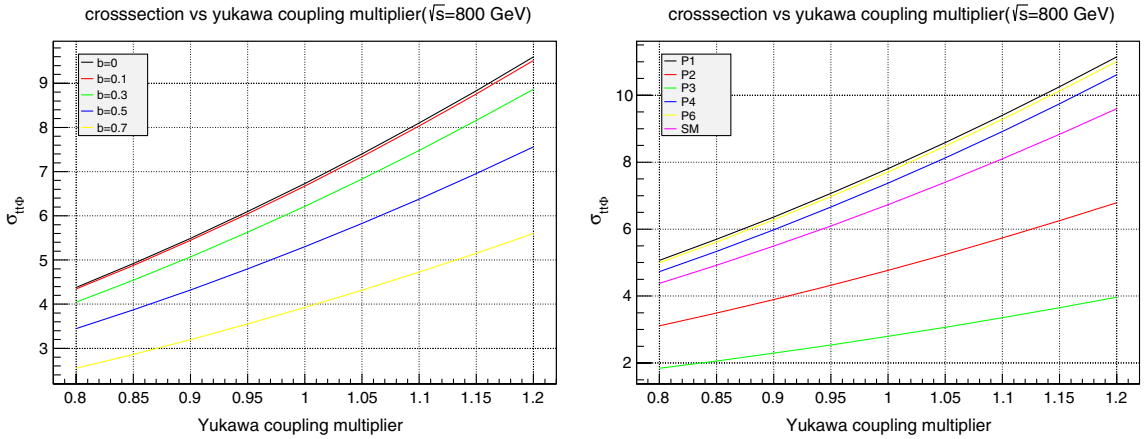

FIG. 3 (color online). $\sqrt{s} = 800$ GeV: $\sigma_{t\bar{t}\Phi}$ vs Yukawa multiplier for different parameter values in model I (left pane) and model II (right panel).

couplings on the prefactor as well as the signal significance. We would like to emphasize that the purpose of this study is to bring home the issues to be addressed while performing Yukawa coupling measurements. We shall also present the decay distributions in order to ascertain the need to adopt different strategies of background reduction. We do not attempt to present a full analysis to evaluate the best sensitivity of the measurements. With ILC, it is a general rule that the beam polarization helps the phenomenology. In the present case, the initial-state polarization does not play a direct role on the final states, except for changed statistics. As already mentioned, in this study we do not perform any analysis to enhance the signal significance. Rather, we rely on the procedure adopted in the earlier rigorous studies made at the respective center-of-mass energies. With this limitation, we follow Ref. [17] and consider an unpolarized beam in the case of a center-of-mass energy of 800 GeV, while for the 500 and 1000 GeV cases beam polarizations are considered as per Refs. [21,23]. It is advisable to include a full detector simulation, exploring the advantages of beam polarization in the analysis to understand the complete picture, which is not attempted in this report.

A. ILC with $\sqrt{s} = 800$ GeV

Top quark Yukawa coupling measurements at the ILC running with unpolarized beams at a center-of-mass energy of 800 GeV were studied in great detail in Ref. [17] for $M_\Phi = 120$ GeV within the SM. While using the realistic detector simulations, they had neglected the effect of Higgs-strahlung off the Z boson, leading to a different extraction method compared to employing Eq. (2), which is considered in more recent studies.

While considering scenarios involving the more general Higgs sector with CP-mixed physical Higgs bosons, we obtained the prefactor for the illustrative parameter choices mentioned above for the two scenarios of model I and model II. The prefactor is obtained from the functional dependence of the cross section on the coupling. In Fig. 3, we present cross-section vs Yukawa-coupling-multiplier curves for model I (left) and model II (right) separately. Here and thereafter, we will not discuss P5, since it has same production cross section value as P4, and thus it will give no different results than P4. The behavior of these curves is expected to fit a quadratic equation $(A\lambda_t^2 + B\lambda_t + C)$, where we define a relative coupling $\lambda_t = \frac{g_t}{g_t^M}$. For easy reference, we follow the representation of Ref. [23] and present the equations of the curves corresponding to different parameter values in Eqs. (11) and (12) below, after fitting the quadratic equation.

$$
\begin{aligned}
b = 0.0&: \ \sigma_{t\bar{t}\Phi} = 6.426(\lambda_t - 1)^2 + 13.040(\lambda_t - 1) + 6.731,\\
b = 0.1&: \ \sigma_{t\bar{t}\Phi} = 6.404(\lambda_t - 1)^2 + 12.933(\lambda_t - 1) + 6.673,\\
b = 0.3&: \ \sigma_{t\bar{t}\Phi} = 5.988(\lambda_t - 1)^2 + 12.049(\lambda_t - 1) + 6.215,\\
b = 0.5&: \ \sigma_{t\bar{t}\Phi} = 5.090(\lambda_t - 1)^2 + 10.280(\lambda_t - 1) + 5.298,\\
b = 0.7&: \ \sigma_{t\bar{t}\Phi} = 3.776(\lambda_t - 1)^2 + 7.632(\lambda_t - 1) + 3.923
\end{aligned}
\tag{11}
$$

and

$$
\begin{aligned}
P1&: \ \sigma_{t\bar{t}\Phi} = 7.470(\lambda_t - 1)^2 + 15.194(\lambda_t - 1) + 7.805,\\
P2&: \ \sigma_{t\bar{t}\Phi} = 4.530(\lambda_t - 1)^2 + 9.189(\lambda_t - 1) + 4.768,\\
P3&: \ \sigma_{t\bar{t}\Phi} = 2.594(\lambda_t - 1)^2 + 5.300(\lambda_t - 1) + 2.796,\\
P4&: \ \sigma_{t\bar{t}\Phi} = 7.367(\lambda_t - 1)^2 + 14.701(\lambda_t - 1) + 7.373,\\
P6&: \ \sigma_{t\bar{t}\Phi} = 7.465(\lambda_t - 1)^2 + 15.031(\lambda_t - 1) + 7.703.
\end{aligned}
\tag{12}
$$

As the equation is an exact quadratic equation, the fit is quite accurate, and the errors on the coefficients can be neglected. We have generically considered them to be

below the per mil level. Please note that P4 and P5 fit to the same equation, as they differ by the sign of the parameter b, which has negligible effect. Therefore, we have not presented the case of P5 in the following. Similarly, the case of P7 is identical to that of P3, and therefore not presented here separately. The value of the prefactor for model I obtained from the above turns out to be 0.516 for the SM value, and it varies very slowly with change in b to be 0.514 for $b = 0.7$. In the case of model II, for P1, P2, and P6 as well, the values of the prefactor remain close to the SM value, giving 0.514, 0.519, and 0.512, respectively. The other points, P3 and P4 show slight deviation from the SM value, leading to 0.528 and 0.502, respectively. The case of P7 is identical to that of P3, again showing that it is the relative sign between a and c that matters, arising through the interference between the two relevant diagrams. By definition, the deviation of the prefactor from the value of $\frac{1}{2}$ indicates the influence of the $ZZ\Phi$ coupling through the Higgs-strahlung contribution to the cross section. As is clear from the parameter values considered, this influence is due to changed values of a and b, rather than the change in c.

The other factor entering Δg_t is the signal sensitivity factor, $\Delta\sigma/\sigma = \sqrt{S+B}/S$. The extraction of this needs signal (S) as well as background (B) events. In order to minimize the background, so as to get the best sensitivity, one employs suitable kinematical cuts and other procedures. The sensitivity also depends on the efficiency of identification of the relevant final states, as well as the efficiency with which events could be reconstructed. Keeping to the limited scope of this study, we will assume the same machine efficiencies and background reduction procedures followed by Ref. [46] in obtaining the sensitivity. The procedure we adopted in our analysis is described below.

The signal events are obtained from the $t\bar{t}\Phi$ production cross section by considering the branching ratios (BRs) appropriate to the specific channels. That is,

$$\sigma^{\text{total}}_{\text{signal}} = \sigma_{t\bar{t}\Phi} \times \text{BR}(t\bar{t} \to X) \times \text{BR}(\Phi \to b\bar{b}), \qquad (13)$$

where X denotes the specific final state corresponding to the hadronic or semileptonic channel, whichever is applicable. We note that, with a CP-indefinite Higgs boson, the decay widths of $\Phi \to b\bar{b}, \tau^+\tau^-, \gamma\gamma, gg, WW^*, ZZ^*$ are all affected, as the $\Phi b\bar{b}$ and ΦVV vertices are all affected. We have taken care of this in obtaining the $\text{BR}(\Phi \to b\bar{b})$. On the other hand, the background remains the same in all cases, as the anomalous vertices do not appear in background processes. We present our results for an assumed integrated luminosity of 1000 fb^{-1}, corresponding to which the total number of signal events in the hadronic and semilepton channels are presented in Table II. Following Ref. [46] in enhancing the signal over the background, the final number of events is also given in Table II, with corresponding reduction factors of 0.234 and 0.235 for the semileptonic and hadronic cases, respectively.

The signal sensitivity and the top quark Yukawa coupling sensitivity for the parameter points of model I and model II are presented in Tables III and IV, respectively. As can be seen, the dominating factor in the sensitivity of the Yukawa coupling measurement is the signal significance,

TABLE II. Total number of events corresponding to $\sqrt{s} = 800$ GeV for an integrated luminosity of 1000 fb^{-1} before and after the kinematical cuts.

No. of events in hadronic case						No. of events in semileptonic case:					
Model I			Model II			Model I			Model II		
b	Total	After cuts	Points	Total	After cuts	b	Total	After cuts	Points	Total	After cuts
0.	399.0	93.8	P1	243.7	57.3	0.	375.4	88.1	P1	229.2	53.8
0.1	396.0	93.1	P2	296.5	69.7	0.1	372.8	87.5	P2	279.1	65.5
0.3	373.5	87.8	P3	163.3	38.4	0.3	351.5	82.5	P3	153.8	36.1
0.5	324.6	76.3	P4	488.4	114.8	0.5	305.5	71.7	P4	459.8	107.9
0.7	247.1	58.1	P6	505.4	118.8	0.7	232.6	54.6	P6	476.0	111.7

TABLE III. Model I: Yukawa coupling sensitivity for different parameters at $\sqrt{s} = 800$ GeV. S_1 and S_2 are signal events in the hadronic and semileptonic modes after kinematical cuts.

b	Prefactor	Signal (S_1)	$\frac{\Delta\sigma}{\sigma}$	$\frac{\Delta g_t}{g_t}$	Signal (S_2)	$\frac{\Delta\sigma}{\sigma}$	$\frac{\Delta g_t}{g_t}$
0.	0.516	93.8	0.17	0.087	88.1	0.18	0.096
0.1	0.515	93.1	0.17	0.088	87.5	0.19	0.097
0.3	0.515	87.8	0.18	0.092	82.5	0.20	0.102
0.5	0.515	76.3	0.20	0.104	71.7	0.22	0.115
0.7	0.514	58.1	0.25	0.131	54.6	0.28	0.146

TABLE IV. Model II: Yukawa coupling sensitivity for different parameters at $\sqrt{s} = 800$ GeV. S_1 and S_2 are signal events in the hadronic and semileptonic modes after kinematical cuts.

Parameter	Prefactor	Signal (S_1)	$\frac{\Delta\sigma}{\sigma}$	$\frac{\Delta g_t}{g_t}$	Signal (S_2)	$\frac{\Delta\sigma}{\sigma}$	$\frac{\Delta g_t}{g_t}$
P1	0.513	57.3	0.26	0.133	53.8	0.29	0.148
P2	0.518	69.7	0.22	0.112	65.5	0.24	0.124
P3	0.527	38.4	0.37	0.196	36.1	0.41	0.220
P4	0.501	114.8	0.14	0.073	107.9	0.16	0.080
P6	0.512	118.8	0.14	0.072	111.7	0.15	0.079

as the prefactor is close to its SM value. In the case of model I, the increasing value of b, which corresponds to the increasing pseudoscalar composition in the Higgs, results in the worsening of the sensitivity monotonously. While for the SM case (model I with $b = 0$), the sensitivity is about 8.7% and 9.6% for the hadronic and semileptonic channels, respectively, it is between 13% and 15% for a pseudoscalar composition of 70%. In the case of model II, in P2 and P3 cases in which a is smaller than unity, the sensitivity is worsened, depending on how small the value of the parameter is. For example, with $a = 0.5$, the sensitivity has gone down to about 20%–22%. On the other hand, the cases of P4 and P6 with $|a| = |b|$ can measure the coupling with a sensitivity of about 7%, which is better than that of the SM case. Meanwhile, in the case of P1, although $a_u = 1.08$, the signal events are small compared to the SM case, because of the reduced BR $(\Phi \to b\bar{b})$ due to a small value of a_d. As mentioned earlier, these variations are mainly due to the changes in the total cross section itself.

In the above, we had assumed that the kinematical cuts that are employed in the case of the SM are applicable in the case with anomalous couplings as well. In reality, the kinematics of the final states could be different in these cases, and therefore, a different strategy may be needed to study the machine capability and signal sensitivity. While it is beyond the scope of this study to present an exhaustive analysis in this regard, we shall present some of the simple kinematic distributions in the cases considered.

Assuming partial reconstruction, we consider two different sets of final states to present the distributions:

(1) Higgs is fully reconstructed: $(e^- e^+ \to t\bar{t}\Phi \to W^+W^- b\bar{b}\Phi)$.
(2) Top quarks are fully reconstructed: $(e^- e^+ \to t\bar{t}\Phi \to t\bar{t}b\bar{b})$.

In order to study the effect of these vertices on kinematical distributions related to the signal process, we present various distributions corresponding to our chosen parameter points for models I and II at 800 GeV. To reduce complexity, we consider the decay of the top and Higgs separately. Thus, we use the following signal processes for the distributions:

$$e^- e^+ \to t\bar{t}\Phi \to W^+W^- b\bar{b}\Phi; \quad t\bar{t}b\bar{b}. \tag{14}$$

We consider the energy, angle, and transverse momentum distributions of the final-state particles in the two models and compare those with the case of the SM. The case of model I is found to have similar behavior for most of the distributions, but with a varying total number of events, as presented earlier. In the case of model II, however, some of the BPs have distinctly different functional dependence than others. To illustrate this, we consider the normalized distributions corresponding to models I and II, and compare them with the respective SM distributions.

In Figs. 4 and 5, we present various distributions corresponding to t and Φ decay for models I and II, resepectively. As is visible from the figures of model I, only $M_{t\bar{t}}$ and E_Φ show a very slight departure from the SM case for a much larger b value of 0.7. However, for model II, except for the benchmark point P3 and in some cases P4, the distributions follow the SM trend. Like in the case of total cross section, the sign of b does not really show up in the distributions as well. While P3 shows perceivable deviation from the rest of the cases in the E_t, M_{tt}, $\cos\theta_{bb}$, E_Φ, M_{WW}, and $(P_T)_\Phi$ distributions, P4 differs from others in the $\cos\theta_t$ and $\cos\theta_W$ distributions. Note that P3 corresponds to the case with a small value of a and a large value of b. Whereas in P3 it is the difference in the magnitude of the parameters that plays the role, in the case of P4 it is the sign of the parameter a that seems to affect the distribution. We must note here that it is in fact the relative sign between a and c that matters, indicating that the interference term between the Higgs-stahlung process with the Higgs radiation off the top-quark is indeed a case of this, as expected. This was confirmed by comparing the results between P6 and P7, which coincide with each other. Thus, the conclusion that we may draw from these analyses is that, while for small deviations from the SM case, the strategy used to obtain the signal sensitivity may be followed, one needs to be cautious in general. We would like to alert the reader that in general, the values of the parameters a and b do not directly relate to the scalar-psuedoscalar mixing. Rather, these parameters could be more complicated functions involving the mixing angle along with other parameters of the model. It is therefore, in principle, possible to have deviations of a and b from the SM values of unity and zero, respectively, even if the Higgs resonance is mostly CP even.

In the rest of this section we shall consider the cases with center-of-mass energies of 500 GeV and 1000 GeV.

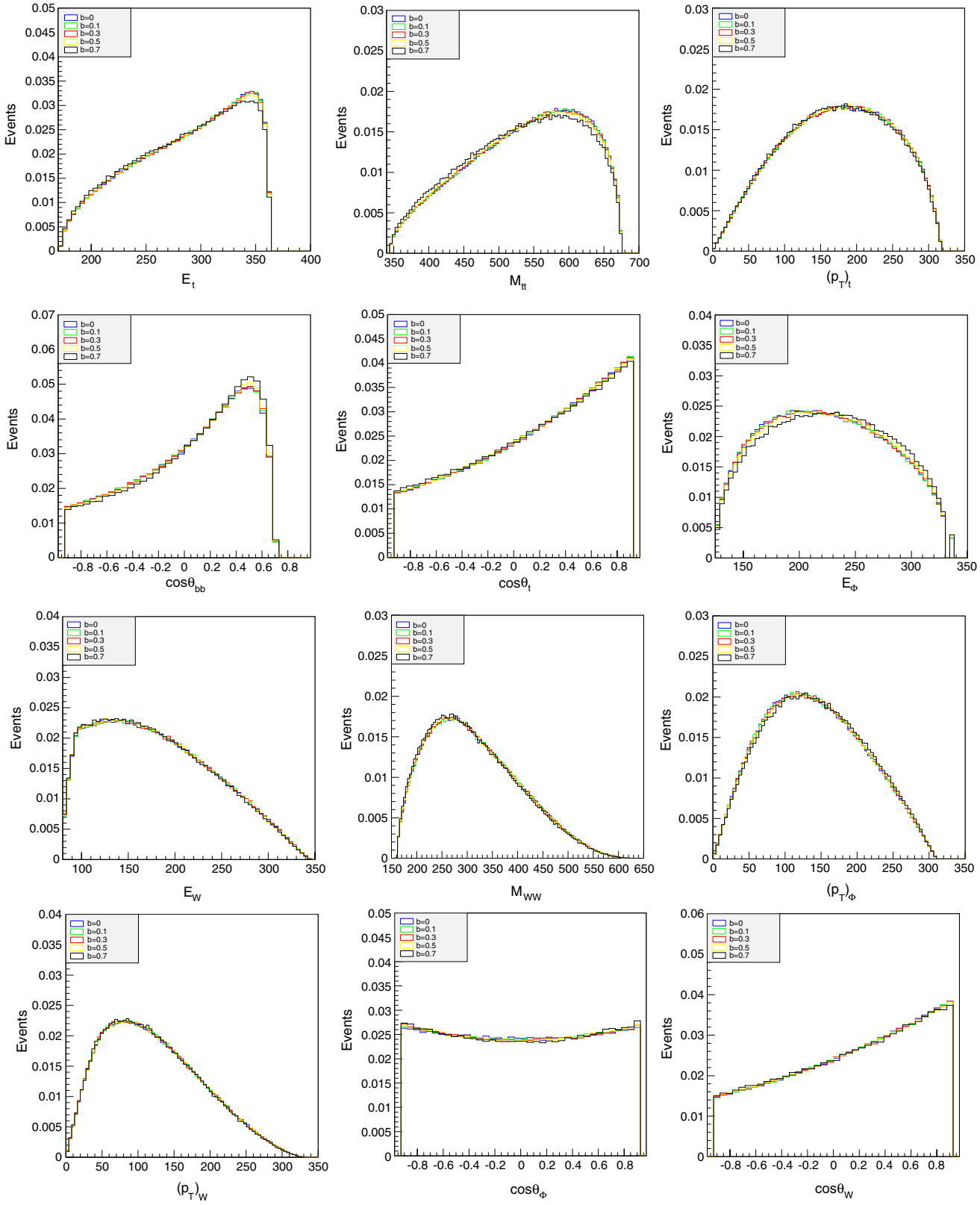

FIG. 4 (color online). Model I: Normalized distributions for the top quark: energy (E_t), $\cos\theta_t$, the invariant mass of $t\bar{t}$ ($M_{t\bar{t}}$), the transverse momentum of t [$(p_T)_t$], and the cosine of the angle between b and $\bar{b}$ in $e^+e^- \to t\bar{t}\Phi \to b\bar{b}t\bar{t}$. For the Higgs boson: energy (E_Φ), transverse momentum [$(p_T)_\Phi$], and $\cos\theta_\Phi$. For the W boson: energy (E_Φ), transverse momentum [$(p_T)_W$], $\cos\theta_W$, and the invariant mass of WW (M_{WW}) in $e^+e^- \to t\bar{t}\Phi \to b\bar{b}W^+W^-\Phi$. The center-of-mass energy considered is $\sqrt{s} = 800$ GeV, and an integrated luminosity of 1000 fb^{-1} is used.

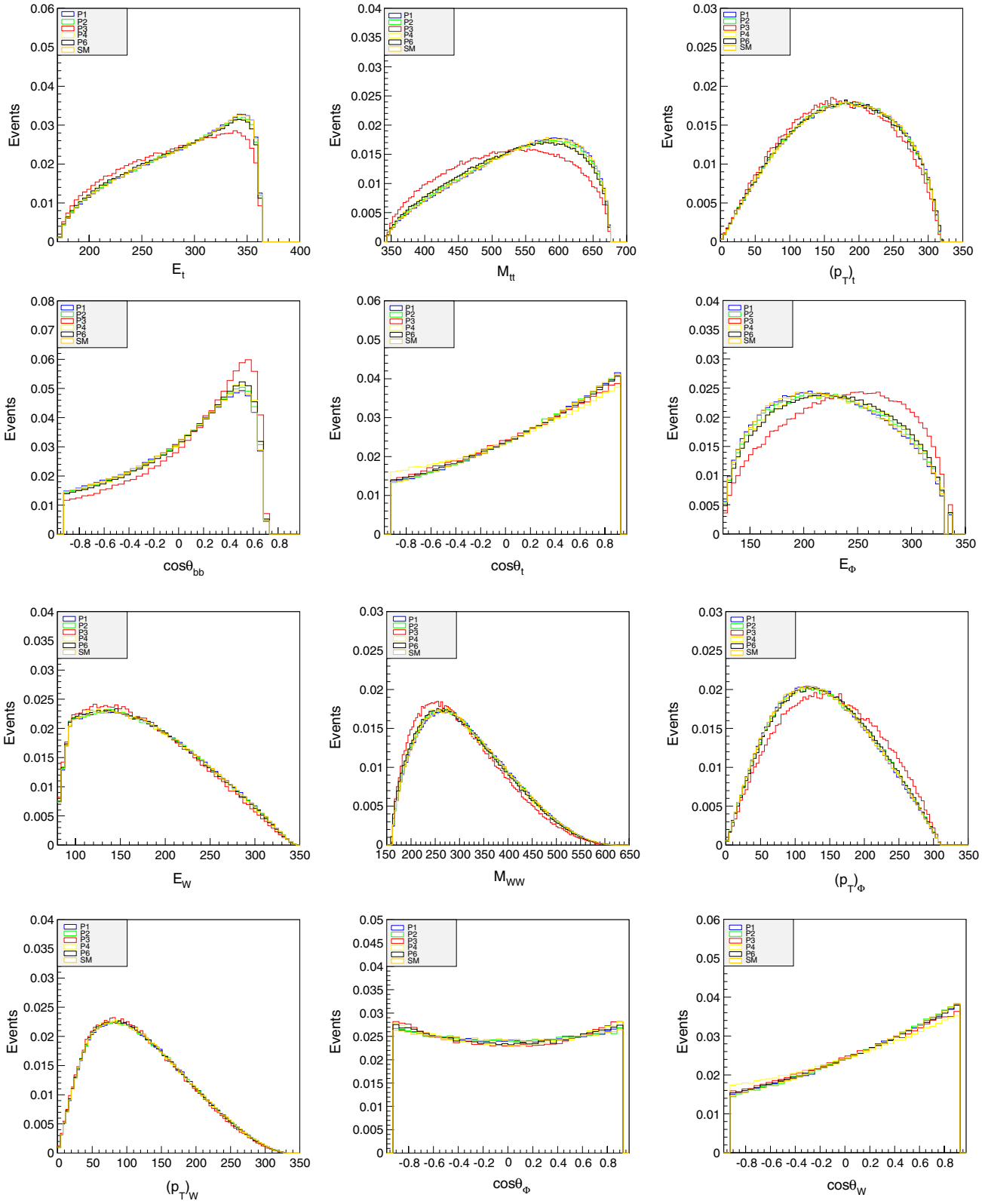

FIG. 5 (color online). Model II: Normalized distributions for the top quark: energy (E_t), $\cos\theta_t$, the invariant mass of $t\bar{t}$ ($M_{t\bar{t}}$), the transverse momentum of t [$(p_T)_t$], and the cosine of the angle between b and $\bar{b}$ in $e^+e^- \to t\bar{t}\Phi \to b\bar{b}t\bar{t}$. For the Higgs boson: energy (E_Φ), transverse momentum [$(p_T)_\Phi$], and $\cos\theta_\Phi$. For the W boson: energy (E_Φ), transverse momentum [$(p_T)_W$], $\cos\theta_W$, and the invariant mass of WW (M_{WW}) in $e^+e^- \to t\bar{t}\Phi \to b\bar{b}W^+W^-\Phi$. The center-of-mass energy considered is $\sqrt{s} = 800$ GeV, and an integrated luminosity of 1000 fb^{-1} is used.

B. $\sqrt{s} = 500$ GeV

This case for SM was studied in Ref. [21] using initial beam polarization with $(P_{e^-}, P_{e^+}) = (-0.8, +0.3)$ and an integrated luminosity of 1000 fb^{-1} for a Higgs mass of $M_\Phi = 120$ GeV. Here we obtained our signal events from WHIZARD for $M_\Phi = 125$ GeV by factorizing the process into its production and decay parts as explained previously. We follow Ref. [21] and work with polarized beams as specified above. This deviation in the treatment compared to the $\sqrt{s} = 800$ GeV case is purely due to the limited scope adopted in this study. As made clear in the earlier sections, our main goal is to illustrate the complications that might arise in the case of a general $t\bar{t}\Phi$ coupling, which is more apt to perform a model-independent investigation. To this effect, we would like to make direct comparisons with the existing detailed study performed strictly within the framework of the SM. A more complete analysis including the advantages of beam polarization over the case of unpolarized beams, with more realistic detector simulations and adopting strategies independent of the ones considered for the SM case, is beyond the scope of this study.

Being close to the threshold, unlike the case of $\sqrt{s} = 800$ GeV, in the present case of $\sqrt{s} = 500$ GeV, $t\bar{t}$ bound-state effects play a significant role, which should be taken care of properly in the signal and background processes. Due to these bound-state effects, the tree-level amplitudes change by a factor [21,47]

$$R_{t\bar{t}} = \frac{A_{t\bar{t}}(i \to f)}{[A_{t\bar{t}}(i \to f)]_{\text{tree}}} = \sqrt{K_{i\to f}} \times F(\hat{s}_{t\bar{t}}, \vec{p}; m_t, \Gamma_t, \alpha_s). \tag{15}$$

Here, F encodes the process-independent bound-state effects, which is a function of the center-of-mass energy of $t\bar{t}$ ($\sqrt{\hat{s}_{t\bar{t}}}$), the three-momentum of t in the CM frame of $t\bar{t}$ ($\vec{p}$), and the pole mass (m_t) and the width (Γ_t) of the top quark. The factor $K_{i\to f}$ is the hard vertex correction factor, which is taken to be 0.843 for the signal, whereas it is considered to be unity for background processes, giving an overall enhancement factor ($R_{t\bar{t}}$) of 1.28 in signal events [21]. Since these effects are independent of the CP parameters, we will use the same factor in our study.

To determine the prefactor, we consider the dependence of the cross section on the Yukawa coupling. In Fig. 6, we present the variation of the cross section with the Yukawa coupling multiplier for our model points. Fitting to the quadratic polynomial leads to the following equations for the respective cases:

$$\begin{aligned}
b = 0.0&: \ \sigma_{t\bar{t}\Phi} = 0.858(\lambda_t - 1)^2 + 1.743(\lambda_t - 1) + 0.881,\\
b = 0.1&: \ \sigma_{t\bar{t}\Phi} = 0.858(\lambda_t - 1)^2 + 1.726(\lambda_t - 1) + 0.872,\\
b = 0.3&: \ \sigma_{t\bar{t}\Phi} = 0.776(\lambda_t - 1)^2 + 1.589(\lambda_t - 1) + 0.803,\\
b = 0.5&: \ \sigma_{t\bar{t}\Phi} = 0.656(\lambda_t - 1)^2 + 1.315(\lambda_t - 1) + 0.665,\\
b = 0.7&: \ \sigma_{t\bar{t}\Phi} = 0.446(\lambda_t - 1)^2 + 0.904(\lambda_t - 1) + 0.457
\end{aligned} \tag{16}$$

and

$$\begin{aligned}
P1&: \ \sigma_{t\bar{t}\Phi} = 1.018(\lambda_t - 1)^2 + 2.031(\lambda_t - 1) + 1.026,\\
P2&: \ \sigma_{t\bar{t}\Phi} = 0.584(\lambda_t - 1)^2 + 1.180(\lambda_t - 1) + 0.597,\\
P3&: \ \sigma_{t\bar{t}\Phi} = 0.226(\lambda_t - 1)^2 + 0.470(\lambda_t - 1) + 0.240,\\
P4&: \ \sigma_{t\bar{t}\Phi} = 0.871(\lambda_t - 1)^2 + 1.739(\lambda_t - 1) + 0.862,\\
P6&: \ \sigma_{t\bar{t}\Phi} = 0.876(\lambda_t - 1)^2 + 1.772(\lambda_t - 1) + 0.895.
\end{aligned} \tag{17}$$

In the SM, the prefactor is 0.50, which means the contribution of the third diagram is negligible. For model I, the prefactor value does not change at all for all considered points. A similar situation persists in model

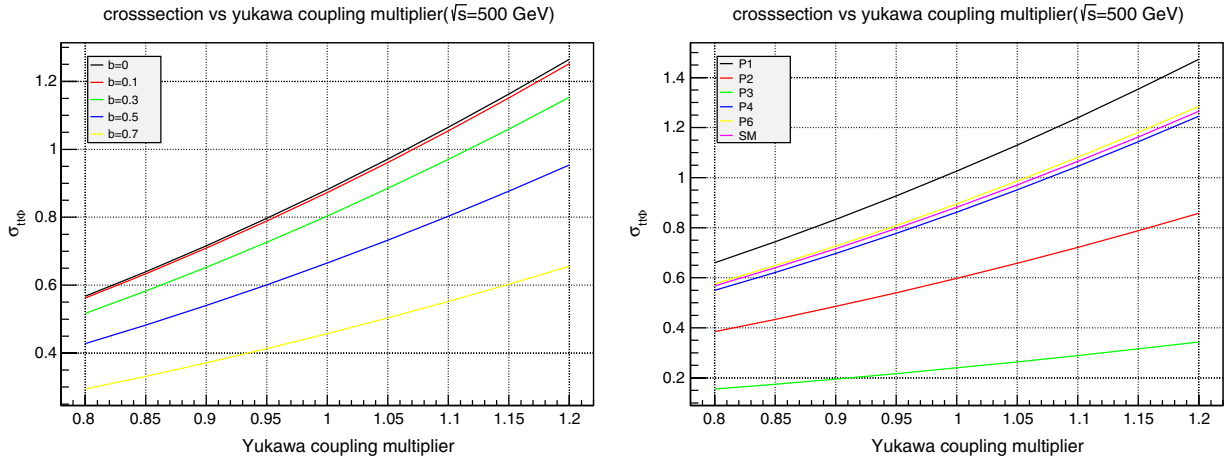

FIG. 6 (color online). $\sqrt{s} = 500$ GeV: $\sigma_{t\bar{t}\Phi}$ vs Yukawa multiplier for different parameter values in model I (left panel) and model II (Right panel).

TABLE V. Model I: Yukawa coupling sensitivity for different parameters at $\sqrt{s} = 500$ GeV. S_1 and S_2 are signal events in the hadronic and semileptonic modes after kinematical cuts.

b	Prefactor	Signal (S_1)	$\frac{\Delta\sigma}{\sigma}$	$\frac{\Delta g_t}{g_t}$	Signal (S_2)	$\frac{\Delta\sigma}{\sigma}$	$\frac{\Delta g_t}{g_t}$
0.	0.505	30.1	0.42	0.214	23.4	0.41	0.207
0.1	0.505	29.8	0.43	0.216	23.2	0.41	0.209
0.3	0.505	27.7	0.46	0.231	21.6	0.44	0.223
0.5	0.505	23.4	0.54	0.270	18.2	0.51	0.259
0.7	0.505	16.6	0.74	0.373	12.9	0.71	0.355

TABLE VI. Model II: Yukawa coupling sensitivity for different parameters at $\sqrt{s} = 500$ GeV. S_1 and S_2 are signal events in the hadronic and semileptonic modes after kinematical cuts.

Parameter	Prefactor	Signal (S_1)	$\frac{\Delta\sigma}{\sigma}$	$\frac{\Delta g_t}{g_t}$	Signal (S_2)	$\frac{\Delta\sigma}{\sigma}$	$\frac{\Delta g_t}{g_t}$
P1	0.505	18.4	0.67	0.339	14.3	0.64	0.323
P2	0.505	21.4	0.58	0.294	16.6	0.56	0.281
P3	0.510	8.0	1.49	0.762	6.2	1.40	0.716
P4	0.495	32.5	0.40	0.198	25.3	0.38	0.192
P6	0.505	33.7	0.38	0.195	26.2	0.37	0.190

II, except for the points P3 and P4, for which its value is 0.51 and 0.49, respectively. Thus, at this center-of-mass energy, the sensitivity of the Yukawa coupling will be governed purely by the $\Delta\sigma/\sigma = \sqrt{S+B}/S$ factor.

As far as the determination of $\Delta\sigma/\sigma$ is concerned, the introduction of various kinematical cuts [21] like mass, b-tagging, thrust, etc., leads to the depletion of signal events by a factor of 0.173 and 0.139 in the hadronic and semileptonic modes, respectively. As emphasized earlier, we will use the same reduction factors for the representative points in our scenarios. The corresponding top Yukawa sensitivity (g_t) with the associated signal significance is given in Tables V and VI for models I and II, respectively. This case gives sensitivity of around 21.4% and 20.7% for hadronic and semileptonic mode in SM. The sensitivity is further dropped to 37.3% and 35.5% for the largest considered mixing $b = 0.7$ in model I. For model II, the best sensitivity of around 19% is obtained in the semileptonic mode for P6, and the worst scenario is for P3, where it reaches 76.2% in the hadronic mode.

C. $\sqrt{s} = 1000$ GeV

This case for SM was considered [23] with a luminosity of 1000 fb^{-1} split equally between two polarization states, $(e^+, e^-) = (\pm 0.2, \mp 0.8)$. The analysis was performed using both a cut-based and a mutlivariate approach. The background events were reduced using a number of selection variables, like the number of isolated events in the sample, the jet clustering algorithm, flavor tagging, the helicity of the $b\bar{b}$ pair associated with Higgs boson, etc.

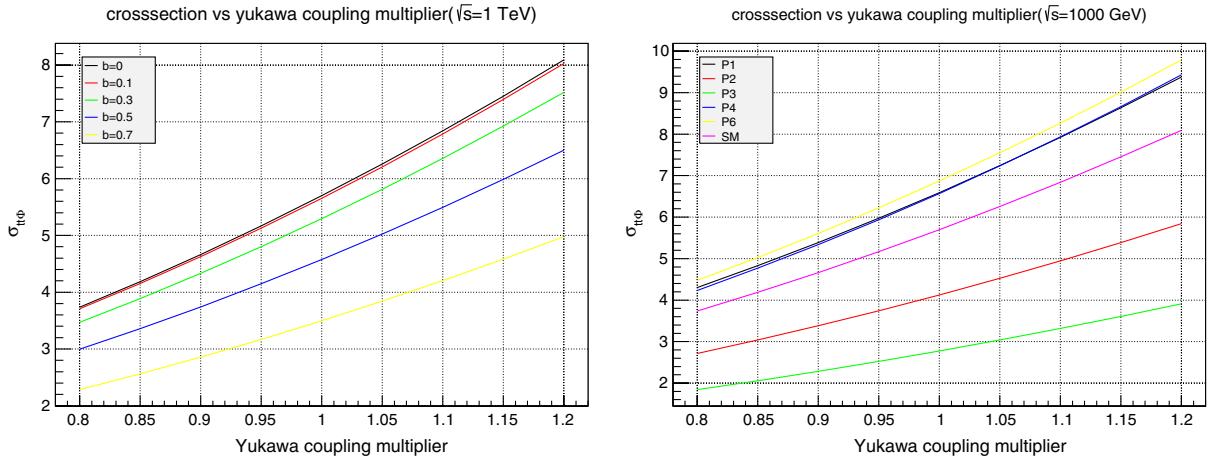

FIG. 7 (color online). $\sqrt{s} = 1000$ GeV: $\sigma_{t\bar{t}\Phi}$ vs Yukawa multiplier for different parameter values in model I (left panel) and model II (right panel).

TABLE VII. Model I: Yukawa coupling sensitivity for different parameters at $\sqrt{s} = 1000$ GeV. S_1 and S_2 are signal events in the hadronic and semileptonic modes after kinematical cuts.

b	Prefactor	Signal (S_1)	$\frac{\Delta\sigma}{\sigma}$	$\frac{\Delta g_t}{g_t}$	Signal (S_2)	$\frac{\Delta\sigma}{\sigma}$	$\frac{\Delta g_t}{g_t}$
0.	0.523	245.4	0.14	0.074	91.3	0.19	0.099
0.1	0.523	243.8	0.14	0.075	90.7	0.19	0.100
0.3	0.522	231.2	0.15	0.079	86.0	0.20	0.104
0.5	0.521	203.6	0.17	0.088	75.8	0.22	0.117
0.7	0.519	160.2	0.21	0.110	59.6	0.27	0.144

TABLE VIII. Model II: Yukawa coupling sensitivity for different parameters at $\sqrt{s} = 1000$ GeV. S_1 and S_2 are signal events in the hadronic and semileptonic modes after kinematical cuts.

Parameter	Prefactor	Signal (S_1)	$\frac{\Delta\sigma}{\sigma}$	$\frac{\Delta g_t}{g_t}$	Signal (S_2)	$\frac{\Delta\sigma}{\sigma}$	$\frac{\Delta g_t}{g_t}$
P1	0.519	148.4	0.22	0.118	55.2	0.29	0.154
P2	0.527	186.8	0.18	0.096	69.5	0.24	0.126
P3	0.536	118.3	0.28	0.152	44.0	0.37	0.196
P4	0.505	313.9	0.11	0.058	116.8	0.15	0.078
P6	0.517	326.2	0.11	0.057	121.4	0.15	0.078

This case gives a signal significance of 7.0 (5.2) and a statistical uncertainty of 7.4%(9.9%) for the hadronic (semileptonic) case on the value of g_t.

Like the previous case, in Fig. 7 we present $\sigma_{t\bar{t}\Phi}$ vs Yukawa coupling multiplier plots for different considered parameter points. The corresponding quadratic equations are given below:

$$\begin{aligned}
b = 0.0&: \ \sigma_{t\bar{t}\Phi} = 5.308(\lambda_t - 1)^2 + 10.884(\lambda_t - 1) + 5.698,\\
b = 0.1&: \ \sigma_{t\bar{t}\Phi} = 5.370(\lambda_t - 1)^2 + 10.800(\lambda_t - 1) + 5.653,\\
b = 0.3&: \ \sigma_{t\bar{t}\Phi} = 4.958(\lambda_t - 1)^2 + 10.123(\lambda_t - 1) + 5.293,\\
b = 0.5&: \ \sigma_{t\bar{t}\Phi} = 4.346(\lambda_t - 1)^2 + 8.767(\lambda_t - 1) + 4.575,\\
b = 0.7&: \ \sigma_{t\bar{t}\Phi} = 3.344(\lambda_t - 1)^2 + 6.733(\lambda_t - 1) + 3.496
\end{aligned} \tag{18}$$

and

$$\begin{aligned}
P1&: \ \sigma_{t\bar{t}\Phi} = 6.250(\lambda_t - 1)^2 + 12.680(\lambda_t - 1) + 6.590,\\
P2&: \ \sigma_{t\bar{t}\Phi} = 3.836(\lambda_t - 1)^2 + 7.822(\lambda_t - 1) + 4.123,\\
P3&: \ \sigma_{t\bar{t}\Phi} = 2.574(\lambda_t - 1)^2 + 5.167(\lambda_t - 1) + 2.772,\\
P4&: \ \sigma_{t\bar{t}\Phi} = 6.637(\lambda_t - 1)^2 + 12.986(\lambda_t - 1) + 6.568,\\
P6&: \ \sigma_{t\bar{t}\Phi} = 6.589(\lambda_t - 1)^2 + 13.286(\lambda_t - 1) + 6.869.
\end{aligned} \tag{19}$$

Here, the SM value of the prefactor is 0.52, which means the third diagram contributes 4% in the total cross section. In model I, the prefactor decreases very slightly with the increase of CP mixing, and its value becomes 0.519 for $b = 0.7$. However, the prefactor changes significantly in model II, and its value is 0.53, 0.50, and 0.51 for P3, P4, and P6, respectively. For P1 and P2 it remains close to the SM value of 0.52.

The introduction of various kinematical cuts [23] for minimizing the background results in the reduction of signal events by factors of 0.391 and 0.151 in the hadronic and semileptonic modes, respectively. The corresponding top Yukawa sensitivity (g_t) with associated signal significance is given in Tables VII and VIII for models I and II, respectively. As observed from these tables, this case provides the best sensitivity for measuring the top Yukawa coupling. It gives a coupling sensitivity of around 7.4% and 9.9% for the hadronic and semileptonic modes in the SM. With nonzero CP violation, the sensitivity is further dropped to 11.0% and 14.4% for largest mixing case ($b = 0.7$) in model I. For model II, the best sensitivity of around 5.7% is obtained in the hadronic mode for P6, while the worst case is for P3, where it reaches about 19.9% in the semileptonic mode.

V. SUMMARY AND CONCLUSIONS

The discovery of the 125 GeV scalar resonance at the LHC opens the way for studying its properties in great detail. Being a hadron collider, the LHC might not fulfill this task completely, which is likely to be followed by a linear collider. On the other hand, the ILC is perceived as a precision machine, which will be crucial in establishing the properties of this new degree of freedom at a very high precision. While the mass and branching ratio measurements of the new resonance, and the spin and parity studies so far, indicate an SM-like Higg boson, the verdict is yet to come in this regard. Moreover, the SM Higgs mechanism is marred with difficulties like the hierarchy problem, which require inputs from beyond the SM. Precise measurement

of the Higgs couplings with all the particles will be the key to understanding what kind of new physics is in store. The top quark, being the heaviest state, couples strongly to the Higgs boson, making a detailed and precise study of the $t\bar{t}\Phi$ coupling essential to help establish the electroweak sector of SM at the energies explored, and at the same time to provide hints of new physics beyond the electroweak energies.

In this work, we have studied the measurement of a general $t\bar{t}\Phi$ coupling, including CP-violating anomalous effects. Such couplings naturally arise in many extensions of the SM, like the 2HDM with CP violation, where the Higgs can be a CP mixture of scalar and pseudoscalar components. We note that, although a pure CP-odd sate is ruled out by the LHC data, the possibility of a mixed CP state is still a viable option, despite perhaps being small.

The issue of the measurement of the Yukawa coupling and the sensitivity achievable at the ILC at the design energies of 500, 800, and 1000 GeV has been the subject of recent studies. In all these, only a SM Higgs was assumed, and it was shown that with typical luminosities of 1000 fb^{-1}, it was possible to achieve sensitivities typically in the range of 10%. At 500 GeV, the issue of bound-state effects was also studied, since the available kinetic energy for the final-state particles is very small. In the present work, we have considered the implication of departing from the SM hypothesis for the Higgs boson. We have considered a generalized coupling and studied the effect on the Yukawa coupling measurements.

It is also important to ask whether the methodology is internally consistent or not. We considered distributions in detail in these models. Our study is validated by the features of these distributions, which is that kinematical cuts affect signal events in the same way for different CP parameters, which is clear from the distributions, and we have used the same reduction factor as for the SM case, which has been studied in the literature.

The main conclusion is that the sensitivity worsens as the departure from the SM grows, partly due to the falling signal cross section, and partly due to different functional dependence of the cross section on the coupling. Assuming the same strategy adopted in the previous studies of the SM case, we find that the measurement of the top Yukawa coupling is possible down to about 20% for 500 GeV energy and 1000 fb^{-1} integrated luminosity in the CP-violating scenario. The case of 800 GeV gives a picture of both improvement as well as worsening of the sensitivity compared to the case of SM, depending on the values of the parameters a and b, ranging between 7% and 22% for different benchmark points considered. The higher energies of about 1000 GeV, show improved significance in general, ranging between 5.7% and about 20%, where the worst case corresponds to the benchmark point P3 with smaller values of the parameter a. To conclude, this first study demonstrates the need for more detailed investigations on the impact of BSM physics on the measurements of the properties of particles at the ILC.

ACKNOWLEDGMENTS

We thank the authors of WHIZARD and the FeynRules interface, especially J. Reuter and C. Speckner, for very helpful discussions regarding the implementation of our models. The work of S. K. G and C. S. K is supported by National Research Foundation of Korea (NRF) Grants No. 2011-0017430 and No. 2011-0020333, funded by the Korean government through the Ministry of Education, Science, and Technology (MEST). P. P. acknowledges the support of BRNS, DAE, and the government of India under Project No. 2010/37P/49/BRNS/1446.

[1] S. Chatrchyan *et al.* (CMS Collaboration), Phys. Lett. B **716**, 30 (2012).
[2] G. Aad *et al.* (ATLAS Collaboration), Phys. Lett. B **716**, 1 (2012).
[3] Atlas Collaboration, Report No. ATLAS-CONF-2013-029, http://cds.cern.ch/record/1527124/files/ATLAS-CONF-2013-029.pdf.
[4] Atlas Collaboration, Report No. ATLAS-CONF-2013-013, http://cds.cern.ch/record/1523699/files/ATLAS-CONF-2013-013.pdf.
[5] Atlas Collaboration, Report No. ATLAS-CONF-2013-031, http://cds.cern.ch/record/1527127/files/ATLAS-CONF-2013-031.pdf.
[6] CMS Collaboration, Report No. HIG-13-002-pas, http://cds.cern.ch/record/1523767/files/HIG-13-002-pas.pdf.
[7] CMS Collaboration, Report No. HIG-13-003-pas, http://cds.cern.ch/record/1523673/files/HIG-13-003-pas.pdf.
[8] F. Maltoni, D. L. Rainwater, and S. Willenbrock, Phys. Rev. D **66**, 034022 (2002).
[9] J. Ellis, D. S. Hwang, K. Sakurai, and M. Takeuchi, J. High Energy Phys. 04 (2014) 004.
[10] J. Chang, K. Cheung, J. S. Lee, and C.-T. Lu, J. High Energy Phys. 05 (2014) 062.
[11] K. Nishiwaki, S. Niyogi, and A. Shivaji, J. High Energy Phys. 04 (2014) 011.
[12] J. Brau *et al.* (ILC Collaboration), arXiv:0712.1950.
[13] G. Aarons *et al.* (ILC Collaboration), arXiv:0709.1893.
[14] G. Moortgat-Pick, T. Abe, G. Alexander, B. Ananthanarayan, A. A. Babich, V. Bharadwaj, D. Barber, A. Bartl *et al.*, Phys. Rep. **460**, 131 (2008).

[15] H. Baer, S. Dawson, and L. Reina, Phys. Rev. D **61**, 013002 (1999).
[16] A. Gay, Linear Collider Note No. LC-PHSM-2006-002.
[17] A. Gay, Eur. Phys. J. C **49**, 489 (2007).
[18] K. Kolodziej and S. Szczypinski, Eur. Phys. J. C **64**, 645 (2009).
[19] K. Kolodziej and S. Szczypinski, Acta Phys. Pol. B **40**, 3015 (2009).
[20] R. Yonamine, K. Ikematsu, S. Uozumi, and K. Fujii, arXiv: 1008.1110.
[21] R. Yonamine, K. Ikematsu, T. Tanabe, K. Fujii, Y. Kiyo, Y. Sumino, and H. Yokoya, Phys. Rev. D **84**, 014033 (2011).
[22] H. Tabassam and V. Martin, arXiv:1202.6013.
[23] T. Price, T. Tanabe *et al.*, Linear Collider Note No. LC-REP-2013-004.
[24] T. Han, T. Huang, Z. H. Lin, J. X. Wang, and X. Zhang, Phys. Rev. D **61**, 015006 (1999).
[25] D. Atwood, S. Bar-Shalom, G. Eilam, and A. Soni, Phys. Rep. **347**, 1 (2001).
[26] B. Grzadkowski and J. F. Gunion, Phys. Lett. B **350**, 218 (1995); J. F. Gunion, B. Grzadkowski and X.-G. He, Phys. Rev. Lett. **77**, 5172 (1996); B. Grzadkowski, J. F. Gunion, and J. Kalinowski, Phys. Rev. D **60**, 075011 (1999); B. Grzadkowski, J. F. Gunion, and J. Kalinowski, Phys. Lett. B **480**, 287 (2000).
[27] A. W. El Kaffas, W. Khater, O. M. Ogreid, and P. Osland, Nucl. Phys. **B775**, 45 (2007); W. Khater and P. Osland, Nucl. Phys. **B661**, 209 (2003); A. Barroso, P. M. Ferreira, R. Santos, and J. P. Silva, Phys. Rev. D **86**, 015022 (2012); J. R. Ellis, J. S. Lee, and A. Pilaftsis, Phys. Rev. D **72**, 095006 (2005).
[28] S. Y. Choi and J. S. Lee, Phys. Rev. D **61**, 015003 (1999); S. Hesselbach, S. Moretti, S. Munir, and P. Poulose, Phys. Rev. D **82**, 074004 (2010); S. Hesselbach, S. Moretti, S. Munir, and P. Poulose, AIP Conf. Proc. **1200**, 498 (2010).
[29] A. Chakraborty, B. Das, J. L. Diaz-Cruz, D. K. Ghosh, S. Moretti, and P. Poulose, arXiv:1301.2745.
[30] M. S. Carena, H. E. Haber, H. E. Logan, and S. Mrenna, Phys. Rev. D **65**, 055005 (2002); **65**, 099902(E) (2002).
[31] P. S. Bhupal Dev, A. Djouadi, R. M. Godbole, M. M. Muhlleitner, and S. D. Rindani, Phys. Rev. Lett. **100**, 051801 (2008).
[32] R. M. Godbole, C. Hangst, M. Muhlleitner, S. D. Rindani, and P. Sharma, Eur. Phys. J. C **71**, 1681 (2011).
[33] S. Bar-Shalom, D. Atwood, G. Eilam, R. R. Mendel, and A. Soni, Phys. Rev. D **53**, 1162 (1996).
[34] S. Berge, W. Bernreuther, and H. Spiesberger, arXiv: 1208.1507.
[35] T. Han and J. Jiang, Phys. Rev. D **63**, 096007 (2001).
[36] K. Rao and S. D. Rindani, Phys. Rev. D **77**, 015009 (2008); **80**, 019901(E) (2009).
[37] J. A. Aguilar-Saavedra, Nucl. Phys. **B821**, 215 (2009).
[38] B. Ananthanarayan, S. K. Garg, J. Lahiri, and P. Poulose, Phys. Rev. D **87**, 114002 (2013).
[39] W. Kilian, T. Ohl, and J. Reuter, Eur. Phys. J. C **71**, 1742 (2011).
[40] N. D. Christensen, C. Duhr, B. Fuks, J. Reuter, and C. Speckner, Eur. Phys. J. C **72**, 1990 (2012).
[41] N. D. Christensen and C. Duhr, Comput. Phys. Commun. **180**, 1614 (2009).
[42] J. S. Lee, M. Carena, J. Ellis, A. Pilaftsis, and C. E. M. Wagner, Comput. Phys. Commun. **180**, 312 (2009).
[43] J. Brod, U. Haisch, and J. Zupan, J. High Energy Phys. 11 (2013) 180.
[44] K. Cheung, J. S. Lee, E. Senaha, and P.-Y. Tseng, arXiv: 1403.4775.
[45] J. Shu and Y. Zhang, Phys. Rev. Lett. **111**, 091801 (2013).
[46] A. Juste and G. Merino, arXiv:hep-ph/9910301.
[47] K. Kolodziej and S. Szczypinski, Acta Phys. Pol. B **38**, 2565 (2007).